Global Journal of Researches in Engineering: A
Mechanical and Mechanics Engineering
Volume 19 Issue 4 Version 1.0 Year 2019
Type: Double Blind Peer Reviewed International Research Journal
Publisher: Global Journals
Online ISSN: 2249-4596 & Print ISSN: 0975-5861

Effect of Aspect Ratio and Installation Direction on Channel Flow Heat Transfer Performance under a wide Range of Reynolds Number

By Shunichi Sakuragi & Daisuke Torii

Abstract- In recent years, in the cooling technology for high-power electronic devices such as power transistors used for drive motor control of electric vehicles and hybrid vehicles, a method of flowing a cooling fluid to a cooling substrate having a fin structure has become the main technology. The structure of the cooling fluid flow path is a channel flow through multiple narrow plate gaps to secure a heat transfer area. In this study, the heat transfer characteristics when the aspect ratio of the channel having a flat rectangular cross-section was changed were investigated in detail by experiments. Moreover, the difference in the heat transfer characteristic at the time of making a rectangular flow path into vertical installation and horizontal installation was also investigated.

Keywords: channel flow, forced convection, natural convection, aspect ratio, synergistic effect, cooling device, power electronics device.

GJRE-A Classification: FOR Code: 091399

Strictly as per the compliance and regulations of:

Effect of Aspect Ratio and Installation Direction on Channel Flow Heat Transfer Performance under a wide Range of Reynolds Number

Shunichi Sakuragi [α] & Daisuke Torii [σ]

Abstract- In recent years, in the cooling technology for high-power electronic devices such as power transistors used for drive motor control of electric vehicles and hybrid vehicles, a method of flowing a cooling fluid to a cooling substrate having a fin structure has become the main technology. The structure of the cooling fluid flow path is a channel flow through multiple narrow plate gaps to secure a heat transfer area. In this study, the heat transfer characteristics when the aspect ratio of the channel having a flat rectangular cross-section was changed were investigated in detail by experiments. Moreover, the difference in the heat transfer characteristic at the time of making a rectangular flow path into vertical installation and horizontal installation was also investigated. As a result, we have clarified the general nature and characteristics of channel flow heat transfer. In particular, in the case of vertical flow, it has been confirmed that the synergetic effect of forced convection and natural convection achieves a maximum heat transfer coefficient in a constant channel width region.

Keywords: channel flow, forced convection, natural convection, aspect ratio, synergistic effect, cooling device, power electronics device.

I. Introduction

With the spread of hybrid vehicles and electric vehicles, the development of a high-efficiency cooling device for high output power electronic devices such as power transistors for controlling high output motors has become one of the important technical issues (Taguchi and Sakuragi, 2014). To achieve high cooling capacity in a limited space volume, it is considered that the design of a cooling system utilizing channel flow is an effective method.

Channel flow is widely used in various cooling devices, heat exchangers, etc., and so far, performance evaluation has been conducted by many experimental studies (Mehta and Khandekar, 2013, Forrest et al., 2014, Ashraf et al., 2016) and simulations on its heat transfer characteristics (Kawamura et al., 2000, Mollik et al., 2017, Uchino et al., 2017). However, there are very few research examples in which heat transfer characteristics are systematically pursued in response to a wide Reynolds number region of the cooling flow and various aspect ratios of the flow channel cross-section. In particular, the optimization of fin thickness and fin spacing is very important to achieve high cooling capacity in a small space (Tanaka et al., 2015). For this purpose, it is also necessary to investigate in detail the effect of the gap width of the channel on the heat transfer performance.

In this study, we fabricated an evaluation system of heat transfer performance that can change the gap width and height of the channel with a rectangular cross-section. And the evaluation data of heat transfer performance were systematically acquired about various channel gap width and aspect ratio. We also acquired data in a wide range of Reynolds numbers of 4,000 to 110,000. Furthermore, the difference in heat transfer characteristics was also evaluated when the channel flow path was placed vertically and horizontally.

From these series of experiments, it was revealed that in the case of the vertically disposed flow passage, there is a flow passage gap width at which the heat transfer coefficient takes a maximum value. In this case, it was confirmed that the heat transfer coefficient could be accurately approximated by a function including both Reynolds number and Grashof number. It is considered that these results obtained in this study can be a useful indicator in the design of high-performance cooling systems for various heat generators.

Nomenclature

D: channel width
d: tube diameter
dh: equivalent diameter of channel cross-section
Gr: Grashof number
H: channel height
L: length of the water-cooled surface of a heat transfer substrate
Nu: Nusselt number
P : static pressure of the flow
Q: flow rate of cooling water
Qa: the amount of heat absorbed by cooling water
Qh: heat generation output of a heater
q: heat flux
Re: Reynolds number
S: heat transfer area
T: temperature

Author α: Department of Mechanical Engineering, Shizuoka Institute of Science and Technology 2200-2 Toyosawa, Fukuroi city, Shizuoka 437-8555, Japan. e-mail: sakuragi.shunichi@sist.ac.jp
Author σ: Yamaha Motor Co., Ltd. 2500 Shingai, Iwata city, Shizuoka 438-8501, Japan.

Tin: temperature of cooling water at the inlet of the test section
Tout: temperature of cooling water at the outlet of the test section
Ts: temperature of the substrate
Tw: temperature of cooling water
W: substrate thickness
α: heat transfer coefficient
λ: thermal conductivity of the substrate
ρ: fluid density

II. Experimental Apparatus and Method

a) Evaluation device of heat transfer performance

Figure 1 shows a schematic diagram of the evaluation device of heat transfer performance. Two pure copper heat transfer substrates are inserted oppositely from both sides of a case made of SUS304, and sandwiching the two spacers at the top and bottom of the substrates, the gap between the two substrates can be adjusted. Five types of gap values *D* (= 1.2, 1.8, 2.4, 3.0, 3.6 mm) were set by the thickness of the spacer.

Two plate heaters (100 V, 200 W) (210 mm × 30 mm × 2 mm in thickness) are attached to the outside of the heat transfer substrate via a heat transfer rubber sheet, and a total heat load of 400 W is generated. Also, three insertion holes for inserting a sheath type thermocouple are provided at equal intervals of 65 mm on the side surface portion of the heat transfer substrate. The substrate temperature at the center of the channel height is measured at a total of six locations on the two substrates, and the substrate average temperature *Ts* (= (*T*1 + *T*2 +.. + *T*6) / 6) is determined. Further, the height *H* of the water-cooled surface of the heat transfer substrate was prepared to be 20 mm and 30 mm. The lengths *L* of the water-cooled surfaces of the heat transfer substrates in the flow direction are all 180 mm.

Figure 2 shows two installation states of the channel flow path. Vertical placement and horizontal placement are shown.

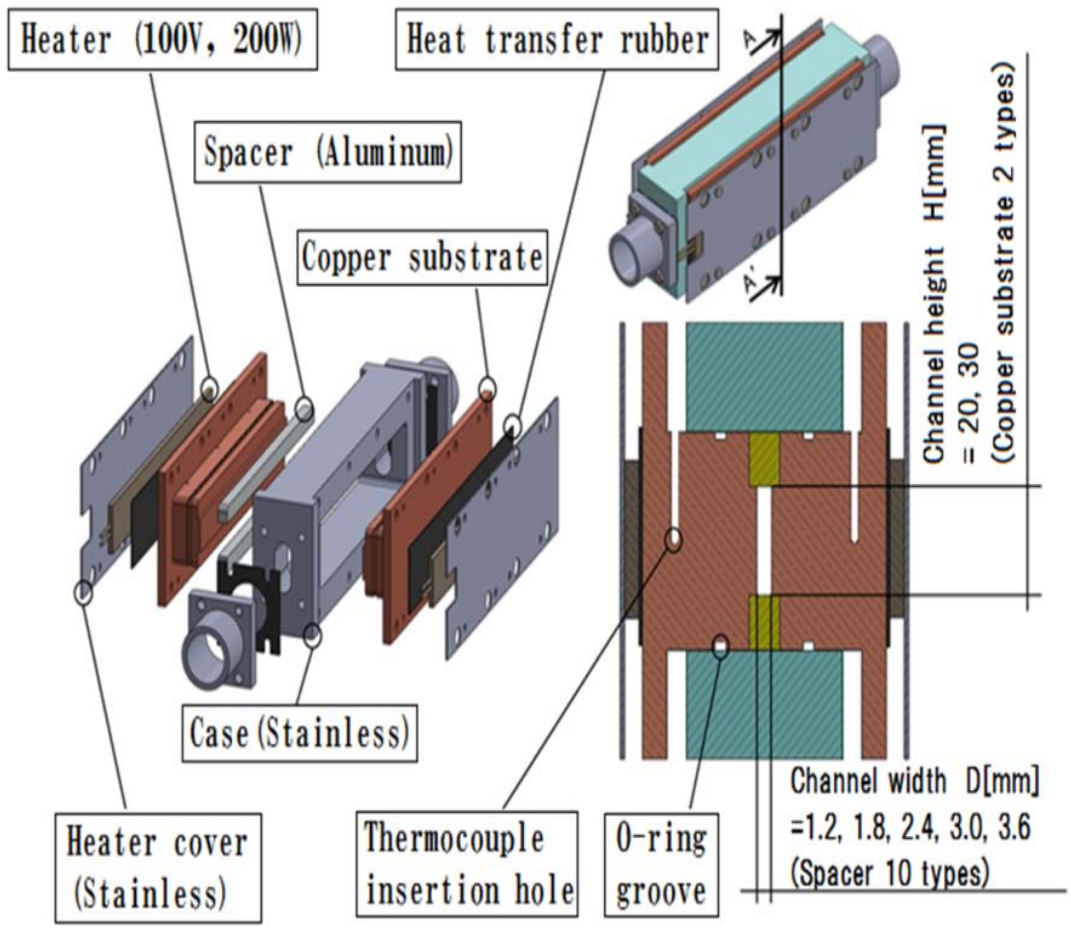

Figure 1: Structure of the evaluation device of heat transfer performance for channel flow.

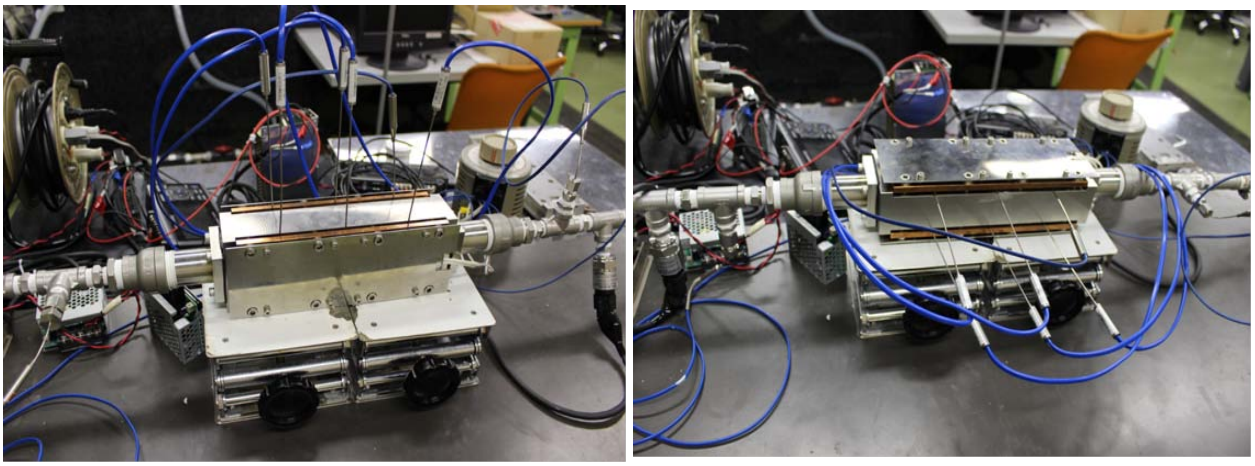

(a) Vertical placement (b) Horizontal placement

Figure 2: Two installation methods of the channel flow path

In this experiment, to obtain an accurate heat transfer coefficient between the cooling water and the substrate, it is necessary to accurately know the substrate surface temperature in contact with the cooling water. In this apparatus, the distance between the heating surface of the substrate and the water-cooled surface is 30 mm, and the substrate temperature is measured at the approximate center of the substrate thickness. Therefore, it is necessary to estimate the difference between the measured temperature and the water cooling surface temperature. The maximum temperature difference is calculated as follows.

In order to estimate the maximum temperature difference ΔT ($= Tsh - Tsw$) between the substrate surface temperature *Tsh* in contact with the heater and the substrate surface temperature *Tsw* in contact with the cooling water, it is assumed that all the heat *Qh* emitted from the heater passes through the water cooling area ($= H \times L$) one-dimensionally. The passing heat flux *q* is calculated by the following equation.

$$q = Q_h / (H\,L) = \lambda\,(\Delta T / W) \quad (1)$$

Here, *Qh* is the heat generation output of the heater (W), *H* is the water-cooled surface height (m), *L* is the water-cooled surface length (m), λ is the substrate thermal conductivity (W / (mK)), *W* is substrate thickness (m). From this, ΔT is calculated as follows.

$$\Delta T = Q_h\,W/(\lambda\,H\,L) = 200\times30\times10^{-3}/(400\times20\times10^{-3}\times180\times10^{-3}) = 4.2\ ^{\circ}\mathrm{C} \quad (2)$$

Therefore, it can be seen that the temperature difference between the measured average temperature Ts and the temperature *Tsw* in contact with the cooling water is about $\Delta T/2 = 2.1$ ℃ at the maximum. In the following discussion, we will consider the measured average temperature Ts as the substrate representative temperature and proceed with the discussion.

b) Configuration of measurement system

Figure 3 shows the measurement system. In the evaluation device of heat transfer performance shown in Fig. 1, water at 20 ℃ is always supplied from the chiller unit, heat is absorbed in the test section, and the heated water is returned to the chiller unit again and cooled.

To accurately estimate the amount of heat absorbed by the cooling water, it is necessary to evaluate the measurement accuracy of the flow meter. This is because the flow meter often has a relatively large measurement error as compared to other sensors.

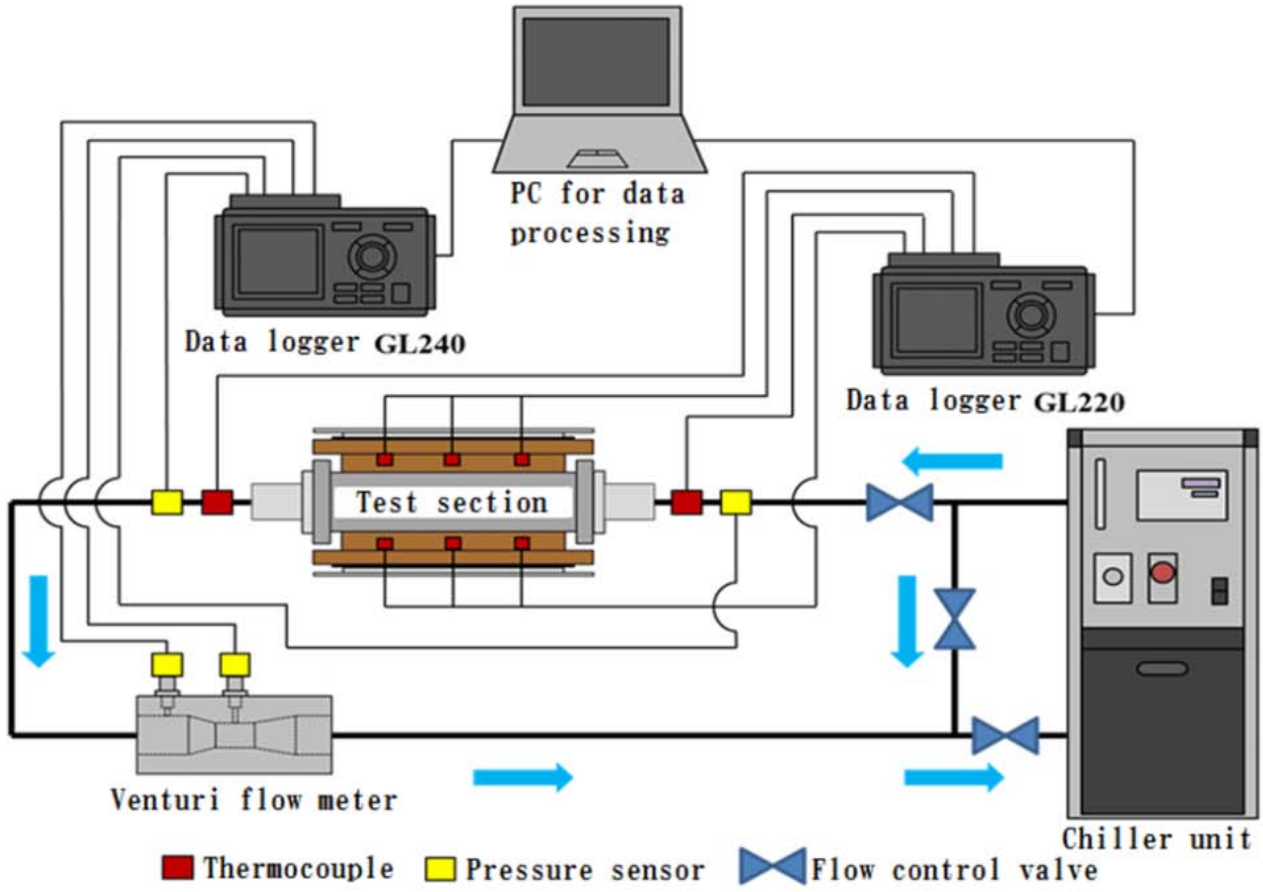

Figure 3: Measurement system for performance data acquisition

The specifications of the Venturi flow meter used in the coolant circuit are shown in Fig. 4. The theoretical flow rate determined from the pressure difference measured by the Venturi flow meter is given by the following equation (Daugherty et al., 1985).

$$Q = \frac{\pi d_1^{\,2}}{4\sqrt{(d_1/d_2)^4 - 1}} \sqrt{\frac{2(P_1 - P_2)}{\rho}} \tag{3}$$

Here, *d*1 and *d*2 represent the pipe diameter of each pressure measurement location.

On the other hand, to investigate the relationship between the actual passing flow rate and the measured pressure difference, the flow rate test was performed by the method shown in Fig. 5. Water was supplied from the tap of the water supply to the inlet of the Venturi flow meter, the passed water was collected with a large beaker, and the time until reaching a predetermined volume was measured to determine the actual flow rate.

The theoretical flow rate and the measured flow rate are plotted in Fig. 6. From the figure, it can be seen that the two match with good accuracy. In the actual flow rate measurement, the method of calculating the flow rate by substituting the pressure difference measured by the Venturi flowmeter into Eq. (3) was adopted.

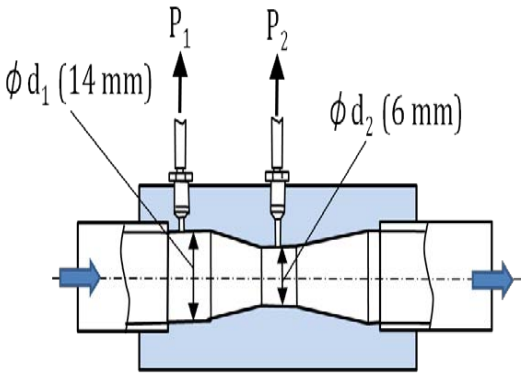

Figure 4: Specifications of the Venturi flowmeter.

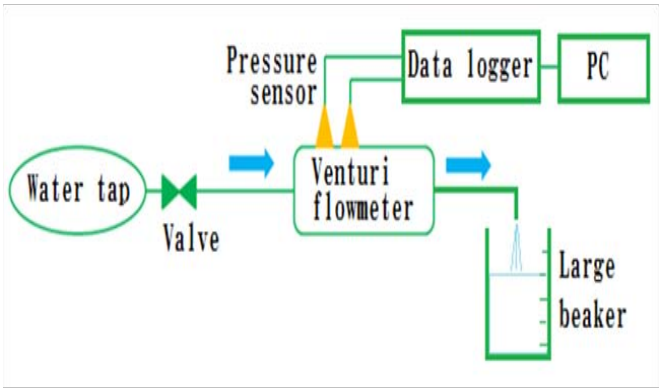

Figure 5: Measurement accuracy verification method of Venturi flow meter

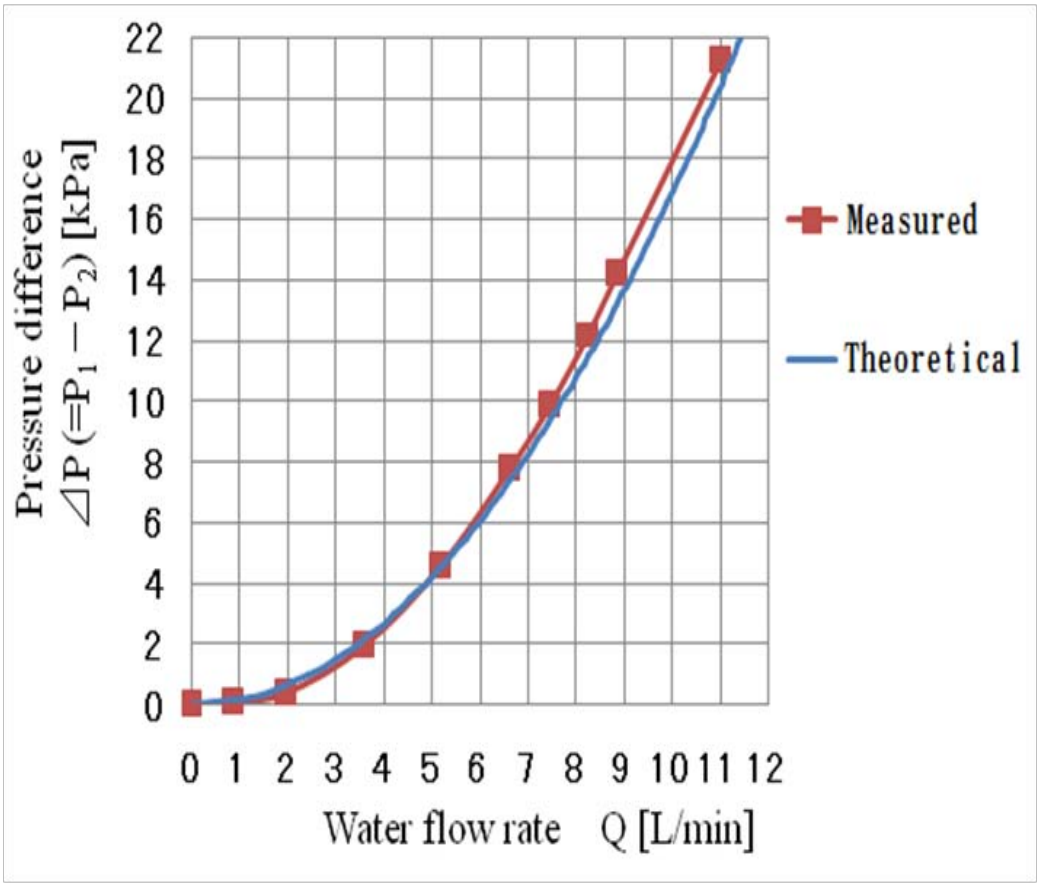

Figure 6: Comparison of the theoretical flow rate of the Venturi flow meter and the measured flow rate

c) Evaluation method of heat transfer performance

The amount of heat Qa absorbed by the cooling water in the test section is expressed by the following equation.

$$Q_a = \dot{m}c(T_{out} - T_{in}) \quad (4)$$

Here, m is the mass flow rate of water, c is the specific heat of water, *Tout* is the temperature of water at the outlet of the test section and *Tin* is the temperature of water at the inlet of the test section.

Further, the average heat transfer coefficient α on the surface of the heat transfer substrate is defined by the following equation.

$$\overline{\alpha} = \frac{Q_a}{S(\overline{T_s} - \overline{T_w})} \quad (5)$$

Here, *S* is a heat transfer area, Tw is average water temperature, and is defined by $Tw = (Tout + Tin) / 2$. Also, the equivalent diameter *dh* of the flow path shape was used as the value of the representative length required for the calculation of the Reynolds number and the Grashof number of the dimensionless parameters related to the heat transfer performance. *dh* is defined by the following formula (Nakayama, 1998).

$$d_h = 2DH/(D+H) \quad (6)$$

Here, *D* is the channel width,and *H* is the channel height (see Fig. 1).

III. Experimental Results and Discussion

a) Amount of heat absorbed by cooling water and substrate temperature

Figures 7 and 8 show the relationship between the flow rate of cooling water and the amount of heat absorbed by cooling water when the channel flow path height *H* is 20 mm and 30 mm, respectively. In each of the graphs, measurement results in the case where the flow path is set vertically and horizontally with the flow path width *D* as a parameter is shown.

In both figures, the larger the flow path width *D*, the larger the absorbed heat amount tends to be. Further, when *H* is 20 mm, the absorbed heat amount is relatively smaller than when *H* is 30 mm, and it is presumed that the amount of heat leakage to the outside of the apparatus is large.

In the case of $H = 20$ mm, no significant difference is observed between the vertical and horizontal placement at any *D* value. However, at $H = 30$ mm, it can be seen that the amount of heat absorbed in the vertical position significantly exceeds the amount of heat absorbed in the horizontal position when $D = 1.8$ and 2.4 mm.

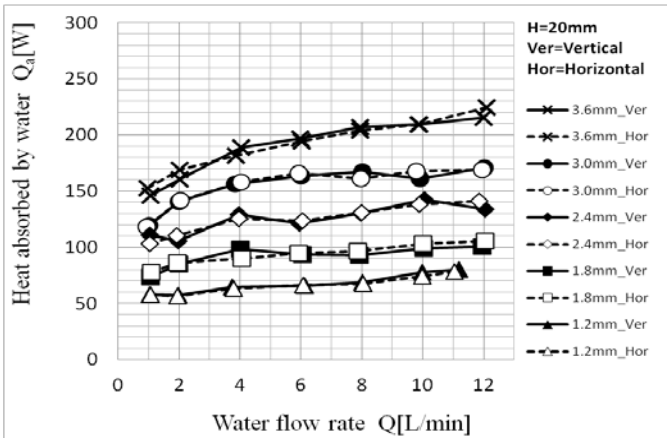

Figure 7: Relationship between cooling water flow rate and absorbed heat quantity (*H*=20mm)

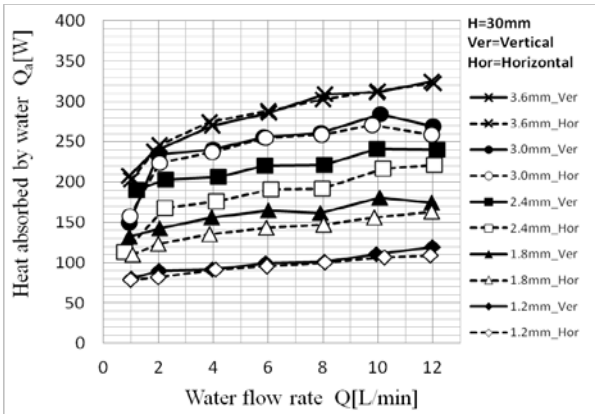

Figure 8: Relationship between cooling water flow rate and absorbed heat quantity (*H*=30mm)

Figures 9 and 10 show the relationship between the cooling water flow rate and the average substrate temperature when the channel height *H* is 20 mm and 30 mm, respectively. In both graphs, the average substrate temperature tends to decrease in inverse proportion to the cooling water flow rate. When *H* is 20 mm, a significant difference between vertical and horizontal placement is not seen. However, when *H* is 30 mm, horizontal placement tends to lower the substrate temperature.

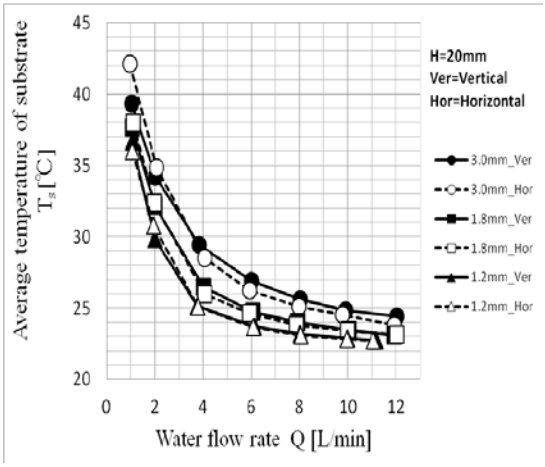

Figure 9: Relationship between cooling water flow rate and average substrate temperature (*H*=20mm)

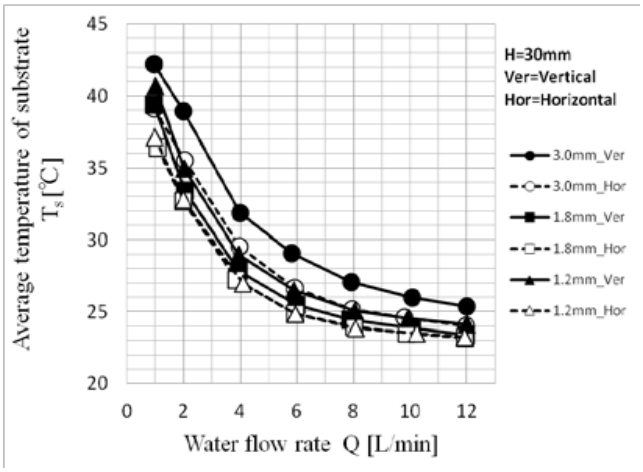

Figure 10: Relationship between cooling water flow rate and average substrate temperature (*H*=30mm).

b) Relationship between Reynolds number of cooling water flow and heat transfer coefficient

Figures 11 and 12 show the relationship between the Reynolds number of the cooling water flow and the average heat transfer coefficient when the channel height *H* is 20 mm and 30 mm, respectively. In both figures, the heat transfer coefficient increases as the *Re* number increases. Also, the larger the value of *D*, the larger the rate of increase.

Comparing Fig. 11 and Fig. 12, it can be seen that when the aspect ratio $D/H = 0.06$, the heat transfer coefficients in the vertical and horizontal placements have the same value over almost all *Re* number regions. At other aspect ratios, the heat transfer coefficient becomes larger in almost all cases when it is placed horizontally.

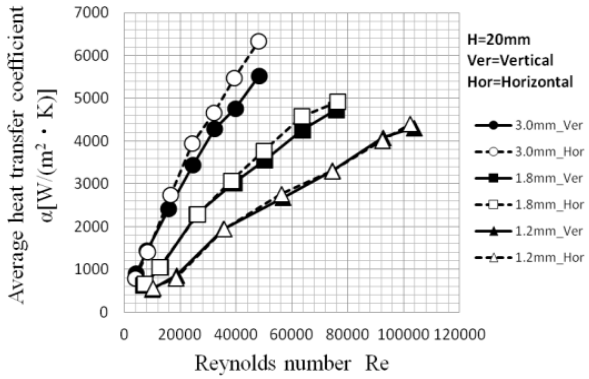

Figure 11: Relationship between *Re* number of flow and average heat transfer coefficient (*H*=20mm)

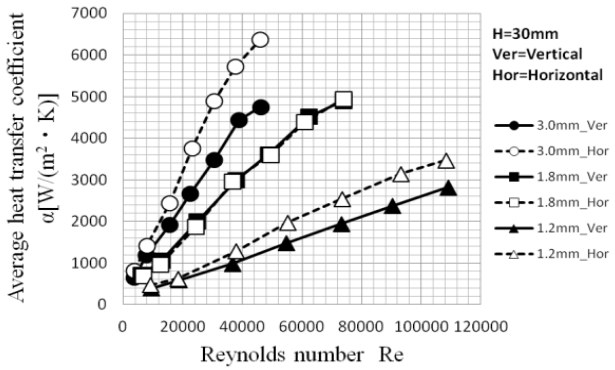

Figure 12: Relationship between *Re* number of flow and average heat transfer coefficient (*H*=30mm)

c) Influence of natural convection effect

Figure 13 shows the relationship between the water flow rate and the *Gr* number when the channel height H = 30 mm. In the case of the channel width D = 1.2 mm and 1.8 mm, the *Gr* number has a substantially constant value regardless of the flow rate. Further, in this case, the *Gr* number values become equal in the vertical placement and the horizontal placement. Therefore, in the case of having these values of D, it is inferred that the influence of natural convection is strongly limited by the influence of strong viscosity. When D is larger than 1.8 mm, the value of the *Gr* number rapidly increases with the decrease of the flow rate, and a difference occurs in the value between the vertical placement and horizontal placement. Also, the same tendency is shown in the case of the flow path height H = 20 mm.

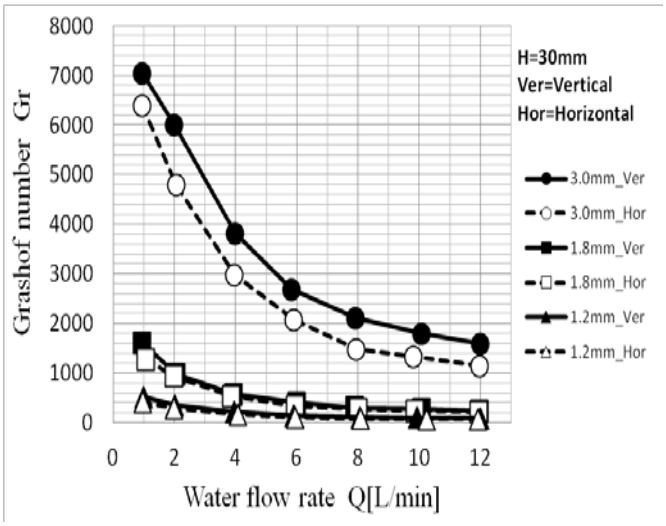

Figure 13: Relationship between cooling water flow rate and *Gr* number.

d) Effects of channel width on the heat transfer coefficient

Figure 14 shows the relationship between the *D* value and the average heat transfer coefficient when cooling water with a constant flow rate is supplied at each channel width when $H = 30$ mm. From the figure, it can be seen that the heat transfer coefficient takes a maximum value at $D = 2.4$ mm in the case of a vertically placed flow. It is also noteworthy that at this *D* value, the value of the heat transfer coefficient is greater at all flow rates than at the horizontally placed flow case.

The peculiar behavior of the heat transfer coefficient observed in the vertical placement is considered to occur in the region where forced convection and natural convection coexist. Therefore, to formulate the heat transfer coefficient in this flow region, it is necessary to obtain a function type including both the Reynolds number and the Grashof number.

It has been found that this heat transfer phenomenon can be approximated relatively well by the following equation in the range of 1.8 mm ≤ *D* ≤ 3.6 mm (see Appendix).

$$\bar{\alpha} = C_1 \cdot C_2 / (Re^{0.5} \cdot Gr^{0.08}) \quad (7)$$

Here, *C*1 is a constant determined by the flow rate *Q*, and *C*2 is a constant determined by the flow path width *D*, and is expressed by the following equations, respectively.

$$C_1 = 0.2Q - 0.3 \quad [\times 10^6 \ \mathrm{W/(m^2K)}] \quad (8)$$

$$C_2 = 0.479D^3 - 3.898D^2 + 10.14D - 7.402 \quad (9)$$

In the above equations, the unit of *Q* is (L/min), and the unit of *D* is (mm). Also, *C*2 is a dimensionless number. The comparison between the values calculated by Eq. (7) and the measured values are shown in Fig.15.

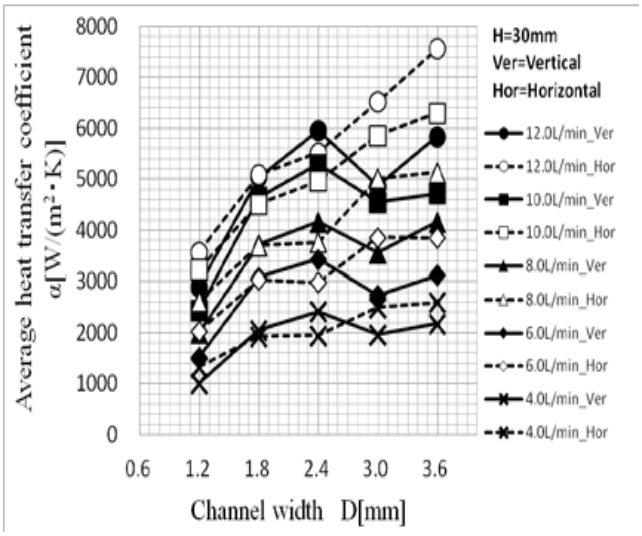

Figure 14: Relationship between channel width and average heat transfer coefficient

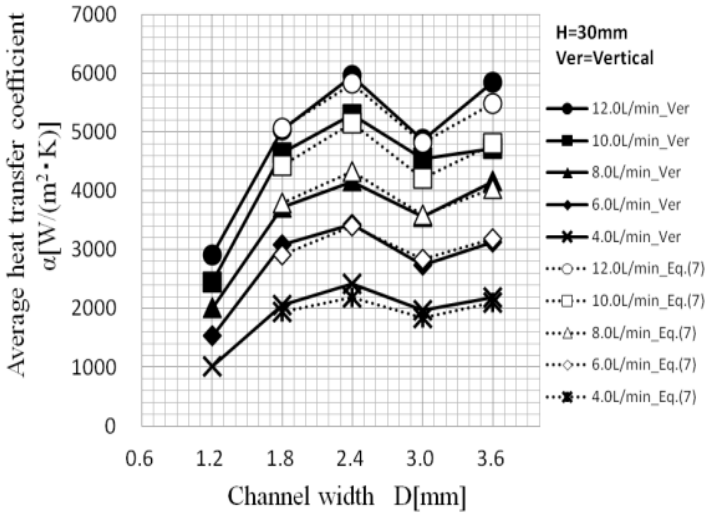

Figure 15: Functional approximation of heat transfer coefficient by Eq. (7) and comparison with the measured values

It is predicted that this unique heat transfer phenomenon is strongly influenced by both *Re* number and *Gr* number. And it is thought that the synergistic effect of forced convection and natural convection appears most effectively in the vicinity of the channel width of 2.4 mm.

In the future, it is desired to clarify the detailed physical mechanism of the heat transfer phenomenon of channel flow approximated by Eq.(7).

As an effective utilization of high heat transfer phenomenon due to mixed convection whose existence has been confirmed in this research, it is expected to be applied to the development of high-performance cooling devices with excellent cooling capacity per volume. This is because in the design of a cooling device composed of a plurality of cooling fins, the optimum design of fin thickness and fin gap width is the most important index governing performance. By determining the optimum fin gap width, the optimum relationship between fin thickness and total heat transfer area can be identified.

IV. Conclusions

In this study, the heat transfer phenomenon in the channel flow was examined in detail by changing the channel width and the channel height by experiment. We also examined the difference between vertical and horizontal placement. The following shows the conclusions obtained in this study.

1. When the aspect ratio of the flow path is $D / H = 0.06$, the heat transfer coefficients in the case of vertical installation and horizontal installation has equal values in a wide *Re* number range.
2. When the channel width is $D = 1.8$ mm or less, the *Gr* number is a small value of an almost constant value independent of the flow rate regardless of vertical and horizontal placement. In this case, it is considered that the effect of the viscous force is very large, and the effect of the natural convection is suppressed to a small value.
3. When a fixed flow rate of cooling water is supplied in a vertical installation, the heat transfer coefficient tends to take maximum value when $D = 2.4$ mm. The vicinity of this flow passage width is considered to be a region where the synergetic effect of forced convection and natural convection appears most effectively, and the phenomenon can be well approximated as a heat transfer coefficient function, including both *Re* number and *Gr* number.

Appendix

About the method for finding the approximation function

The heat transfer characteristics on a flat plate are generally expressed by the following equations when the change of the Prandtl number of the cooling fluid due to temperature is small. That is, forced convection heat transfer is expressed by the Eq. (A1), and natural convection heat transfer is expressed by the Eq. (A2) (Chapman, 1987).

$$Nu = k_1 Re^m \quad (k_1, m : \text{constant}) \tag{A1}$$

$$Nu = k_2 Gr^n \quad (k_2, n : constant) \tag{A2}$$

The formulation of the phenomena that natural convection heat transfer and forced convection heat transfer are thought to coexist is assumed as the following equation.

$$Nu = k_3 Re^s Gr^t \quad (k_3, s, t : \text{constant}) \tag{A3}$$

Accordingly, the average heat transfer coefficient α is expressed by the following equation.

$$\overline{\alpha} = C Re^x Gr^y \quad (C, x, y : \text{constant}) \tag{A4}$$

Next, the coefficients *C*, *x*, and *y* in the Eq. (A4) are determined to perform curve fitting with a minimum error as compared with the measured value of the average heat transfer coefficient.

As the first step, at each flow rate *Q*, when the value of α in equation (A4) matches the measured value in the range of 1.8 mm $\leq D \leq$ 3.6 mm, the values of *x* and *y* were determined to satisfy the condition that the value of *C* is constant without depending on the value of *D*. As a result, it was found that when the values of *x* and *y* are represented by Eq. (A5) at all flow rates, the value of *C* corresponding to each *D* value takes a minimum error. The results are shown in Table A1.

$$(x, y) = (-0.5, -0.08) \tag{A5}$$

Table A1: Value of *C* at each flow rate [(x,y) = (-0.5, -0.08)]

		D [mm]	1.8	2.4	3.0	3.6	Average
Q [L/min]	4.0	C [$\times 10^6$ W/(m^{2}K)]	0.524	0.599	0.466	0.493	0.521
	6.0		0.942	0.987	0.751	0.837	0.879
	8.0		1.261	1.354	1.120	1.269	1.251
	10.0		1.765	1.894	1.594	1.583	1.709
	12.0		2.066	2.328	1.841	2.119	2.089

In the data of Table A1, when the relationship between the average value of *C* and the flow rate *Q* is graphed, it becomes as shown in Fig. A1, and it can be understood that *C* can be approximated by a linear function of *Q*. That is,

$$C \approx f(Q) = 0.2Q - 0.3 \qquad [\times 10^6\ \mathrm{W/(m^2K)}] \qquad \text{(A6)}$$

Next, we compare the measured average heat transfer coefficient and the average heat transfer coefficient calculated from the Eq. (A4) using the values of *x*, *y*, and *C* defined by the Eq. (A5) and Eq. (A6). The results are shown in Fig. A2.

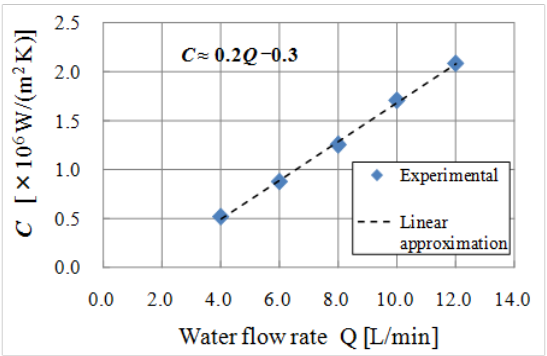

Figure A1: Relationship between the water flow rate *Q* and the average value of *C*

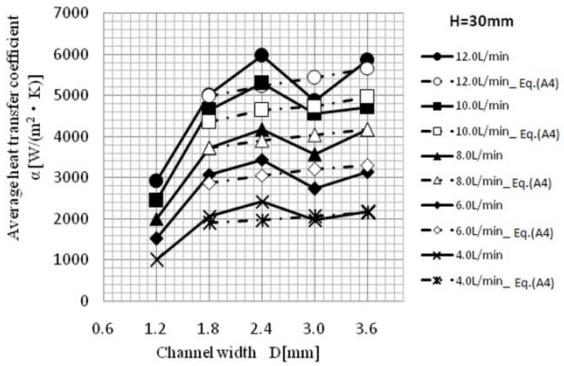

Figure A2: Comparison of the values calculated by the Eq. (A4) with the measured values

From the figure, it can be seen that the result calculated using the value of *C* determined by the Eq. (A6) shows a set of average values of heat transfer coefficients in the range of 1.8 mm ≤ D ≤ 3.6 mm.

Therefore, *C* should be considered as a coefficient determined by the two factors of the flow rate *Q* and the flow path width *D* in order to make the approximation of the heat transfer coefficient more accurate. That is,

$$C = C_1 \cdot C_2 = f(Q) \cdot g(D) \qquad \text{(A7)}$$

However, it is

$$C_1 = f(Q) = 0.2Q - 0.3\,[\times 10^6\ \mathrm{W/(m^2K)}] \qquad \text{(A8)}$$

Here, the values of *C*2 = *C* / *C*1 = *C* / *f* (*Q*) are as shown in the following Table A2.

Table A2: Value of C_2 at each channel width *D*.

		D [mm]	1.8	2.4	3.0	3.6
Q [L/min]	4.0	$C_2 = C/C_1$	1.048	1.199	0.931	0.987
	6.0		1.046	1.096	0.835	0.930
	8.0		0.970	1.041	0.862	0.976
	10.0		1.038	1.114	0.937	0.931
	12.0		0.984	1.109	0.877	1.009
		Average	1.017	1.112	0.888	0.967

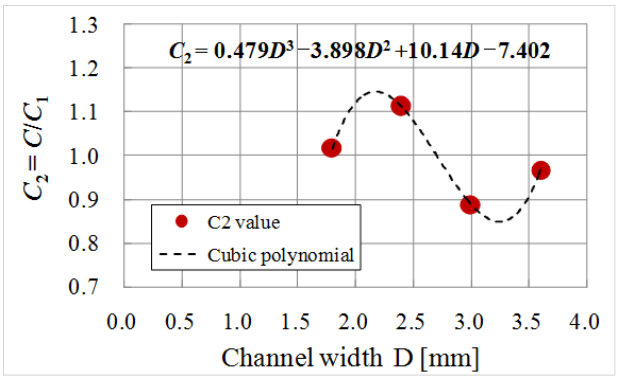

Figure A3: Relationship between the mean value of *C*2 and channel width *D*

Figure A3 plots the relationship between the mean value of *C*2 and *D*, and approximates it with a third-order polynomial. From this, the approximate expression of *C*2 is expressed as the following equation.

$$C_2 = g(D) = 0.479D^3 - 3.898D^2 + 10.14D - 7.402 \quad \text{(A9)}$$

From the above, *C*1 and *C*2 can be expressed by the Eq. (8) and Eq. (9) respectively, and an approximate expression of the average heat transfer coefficient in the flow path width range 1.8mm ≤ D ≤ 3.6mm can be expressed by the Eq. (7).

References Références Referencias

1. Ashraf, A., Mohammed, S. N., Thoufeeq, A., Bibin, S. and Arun, S., Experimental Analysis of Performance Characteristics of Mini Channel Heat Exchangers, International Journal of Research in Mechanical Engineering, Vol. 4, Issue 3, (2016), pp. 39–43.
2. Chapman, A. J., Fundamentals of heat transfer (1987), pp. 311–379, Macmillan.
3. Daugherty, R. L., Franzini. J. B. and Finnemore, E. J., Fluid Mechanics with Engineering Applications, eighth edition (1985), p. 420, Mc Graw-Hill.
4. Forrest, E. C., Hu, L. W., Buongiorno, J. and McKrell, T. J., Convective Heat Transfer in a High Aspect Ratio Mini-Channel Heated on One Side, Journal of Heat Transfer, SAND2014-18834J, pp. 1–57.
5. Kawamura, H., Abe, H. and Shingai, K., DNS of turbulence and heat transport in a echannel flow with different Reynolds and Prandtl numbers and boundary conditions, Proceedings of the 3rd Int. Symp. on Turbulence, Heat and Mass Transfer, (2000), pp. 1–18.
6. Mehta, B. and Khandekar, S., Local experimental heat transfer of single-phase pulsating flow in a square mini-channel, Proceedings of the ASME 2013 4th Micro/Nanoscale Heat & Mass Transfer International Conference, pp. 1–7.
7. Mollik, T., Roy, B. and Saha, S., Turbulence modeling of channel flow and heat transfer: A comparison with DNS data, 10th International Conference on Marine Technology, ELSEVIER Procedia Engineering 194 (2017), PP. 450–456.
8. Nakayama, Y., Dynamics of fluid (revised edition) (1998), p. 107, Youkendou (in Japanese).
9. Taguchi, T. and Sakuragi, S., Experimental study on high efficiency cooling mechanism of power electronic devices, Proceedings of the 1st IPEJ Chubu District Conference on Research achievements, (2014), pp. 17 20 (in Japanese).
10. Tanaka, Y., Yamaji, K. and Sakuragi, S., Optimization study of cooling substrate fin structure, Proceedings of the 2nd IPEJ Chubu District Conference on Research achievements, (2015), pp. 5–8 (in Japanese).
11. Uchino, K., Mamori, H. and Fukagata, K., Heat transfer in fully developed turbulent channel flow with streamwise traveling wave-like wall deformation, Journal of Thermal Science and Technology, Vol.12, No.1 (2017), pp.1–11.